

# Casting Light on Dark Matter

John Ellis

CERN-PH-TH/2011-141, KCL-PH-TH/2011-18, LCTS/2011-03

**Abstract** The prospects for detecting a candidate supersymmetric dark matter particle at the LHC are reviewed, and compared with the prospects for direct and indirect searches for astrophysical dark matter. The discussion is based on a frequentist analysis of the preferred regions of the Minimal supersymmetric extension of the Standard Model with universal soft supersymmetry breaking (the CMSSM). LHC searches may have good chances to observe supersymmetry in the near future - and so may direct searches for astrophysical dark matter particles, whereas indirect searches may require greater sensitivity, at least within the CMSSM.

**Keywords** Dark matter · LHC · Supersymmetry

## 1 Introduction

The standard list of open questions beyond the Standard Model of particle physics [1] includes the following. (1) What is the origin of particle masses and, in particular, are they due to a Higgs boson? (2) Why are there so many different flavours of standard matter particles, e.g., three neutrino species? (3) What is the dark matter in the Universe? (4) How can we unify the fundamental forces? (5) Last but certainly not least, how may we construct a quantum theory of gravity? Each of these questions will be addressed, in some way, by experiments at the LHC, though answers to all of them are not guaranteed! I

---

The work described here was supported partly by the London Centre for Terauniverse Studies (LCTS), using funding from the European Research Council via the Advanced Investigator Grant 267352.

---

J. Ellis

TH Division, Physics Department, CERN, CH-1211 Geneva 23, Switzerland, & Theoretical Particle Physics and Cosmology Group, Physics Department, King's College London, London WC2R 2LS, UK

E-mail: John.Ellis@cern.ch

would argue that supersymmetry is capable of casting important light on all but one of these questions, the exception being that of flavour. As you can guess from the title of this talk is, its focus is on question (3) concerning dark matter and, in light of the above comments, specifically on ways to probe experimentally supersymmetric models of dark matter. These include searches at the LHC as well as astrophysical dark matter searches, and the presentation is based on my personal research in these areas: I apologize to others for not mentioning adequately their work, which is referred to in the papers referenced here.

## 2 Supersymmetric Models

Supersymmetry is a very beautiful theory that is unique in its ability to link bosons and fermions and hence, in principle, force and matter particles. However, phenomenological interest in looking for supersymmetry was sparked by the realization that it could stabilize the electroweak scale if supersymmetric partners or Standard Model particles weigh  $\sim 1$  TeV, and the flames of enthusiasm were fanned by the subsequent realizations that in this case it could also facilitate unification of the fundamental interactions, would predict a light Higgs boson, and could explain the apparent discrepancy between the experimental value of  $g_\mu - 2$  and theoretical calculations within the Standard Model [1]. Moreover, there are general arguments that a dark matter particle that was once in equilibrium in the early Universe, such as the lightest supersymmetric particle (LSP) [2] would naturally have the right density to provide dark matter if it weighed  $\sim 1$  TeV.

The LSP is stable in many supersymmetric models because of the multiplicative conservation of  $R$ -parity, where  $R = (-1)^{2SL+3B}$ ,  $S$  denotes spin, and  $L$  and  $B$  are the lepton and baryon numbers. It is easy to check that Standard Model particles all have  $R = +1$ , whereas their supersymmetric partners would have  $R = -1$ . Multiplicative  $R$  conservation would imply that sparticles must be produced in pairs, heavier sparticles must decay into lighter sparticles, and therefore the lightest supersymmetric particle (LSP) must be stable, and present in the Universe today as a relic from the Big Bang. The LSP should have neither an electric charge nor strong interactions, but should have only weak interactions. It is often thought to be the lightest neutralino  $\chi$ , a mixture of the supersymmetric partners of the photon,  $Z$  boson and neutral Higgs bosons, and this identification will be assumed in the following. There are other possibilities such as the gravitino, which would be difficult to detect astrophysically, but could also have distinctive signatures at the LHC.

We work within the framework of the minimal supersymmetric extension of the Standard Model (MSSM), in which the known particles are accompanied by their simple supersymmetric partners and there are two Higgs doublets, with a superpotential coupling denoted by  $\mu$  and a ratio of Higgs v.e.v.s denoted by  $\tan\beta$  [3]. The bugbear of the MSSM is supersymmetry breaking, which may be parameterized generically through scalar masses  $m_0$ , gaugino

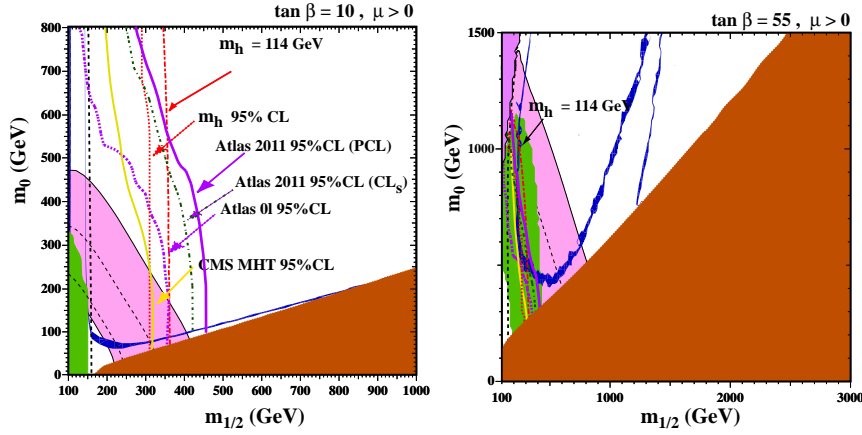
fermion masses  $m_{1/2}$ , trilinear soft scalar couplings  $A_0$  and bilinear soft scalar couplings  $B_0$ . In our ignorance about them, the total number of parameters in the MSSM exceeds 100! For simplicity, it is often assumed that these parameters are universal at the scale of grand unification, so that there are common soft supersymmetry-breaking parameters  $m_0, m_{1/2}, A_0$ , a scenario called the constrained MSSM (CMSSM) [4].

Fig. 1 shows a compilation of theoretical, phenomenological, experimental and cosmological constraints in two  $(m_{1/2}, m_0)$  planes of the CMSSM, taking as examples  $\tan\beta = 10, 55$  and  $A_0 = 0$ . (This plot updates the planes shown previously in [5, 6]. In addition to the absence of a stable charged sparticle (which excludes regions at large  $m_{1/2}$  and small  $m_0$ ) and the presence of a consistent electroweak vacuum (which excludes regions at small  $m_{1/2}$  and large  $m_0$ ), these constraints include the absences of supersymmetric particles at LEP (which require any charged sparticle to weigh more than about 100 GeV [7]), and at the Tevatron collider (which has not found any squarks or gluinos lighter than about 400 GeV [8]). There are also important indirect constraints implied by the LEP lower limit on the Higgs mass of 114.4 GeV [9], and the agreement of the Standard Model prediction for  $b \rightarrow s\gamma$  decay with experimental measurements. The only possible strong experimental discrepancy with a Standard Model prediction is for  $g_\mu - 2$  [10], though the significance of this discrepancy is still uncertain. However, astrophysics provides a clear discrepancy with the Standard Model, since dark matter cannot be explained without physics beyond the Standard Model, such as supersymmetry. The fact that the dark matter density is constrained to within a range of a few percent [11]:

$$\Omega_{DM} = 0.111 \pm 0.006 \quad (1)$$

constrains some combination of the parameters of any dark matter model also to within a few percent, e.g., the parameters  $(m_{1/2}, m_0)$  of the CMSSM for fixed values of its other parameters.

In a series of papers [15, 16, 17], we have made global fits to the parameters of various supersymmetric models, including those of the CMSSM, in a frequentist approach incorporating precision electroweak data, the LEP Higgs mass limit,  $\Omega_{DM}$ , data on the B decays  $b \rightarrow s\gamma$ ,  $B^\pm \rightarrow \tau^\pm \nu$  and  $B_s \rightarrow mu^+ \mu^-$ , and (optionally)  $g_\mu - 2$ . One example of a pre-LHC frequentist fit within the CMSSM is shown in Fig. 2 [15], where the estimated reaches of the LHC experiments with various centre-of-mass energies and integrated luminosities are indicated. These give cause for hope to discover supersymmetry in the early days of the LHC, and we discuss later the implications of the first LHC searches. The primary signals being sought at the LHC are events with missing transverse energy carried off by dark matter particles, accompanied by hadronic jets and possibly leptons.



**Fig. 1** The  $(m_{1/2}, m_0)$  planes in the CMSSM for  $\tan \beta = 10$  (left) and  $\tan \beta = 55$  (right), assuming  $\mu > 0$  and  $A_0 = 0$  [5,6], showing the 95% CL limits imposed by ATLAS [12,13] and CMS [14] data (purple and yellow lines, respectively). The regions where the relic LSP density falls within the range allowed by WMAP [11] and other cosmological observations appear as strips shaded dark blue. The constraints due to the absences of charginos [7] and the Higgs boson [9] at LEP are also shown, as black dashed and red dot-dashed lines, respectively. Regions excluded by the requirements of electroweak symmetry breaking and a neutral LSP are shaded mauve and brown, respectively. The green region is excluded by  $b \rightarrow s\gamma$ , and the pink region is favoured by the supersymmetric interpretation of the discrepancy between the Standard Model calculation and the experimental measurement of  $g_\mu - 2$  [10] within  $\pm 1$  and  $\pm 2$  standard deviations (dashed and solid lines, respectively).

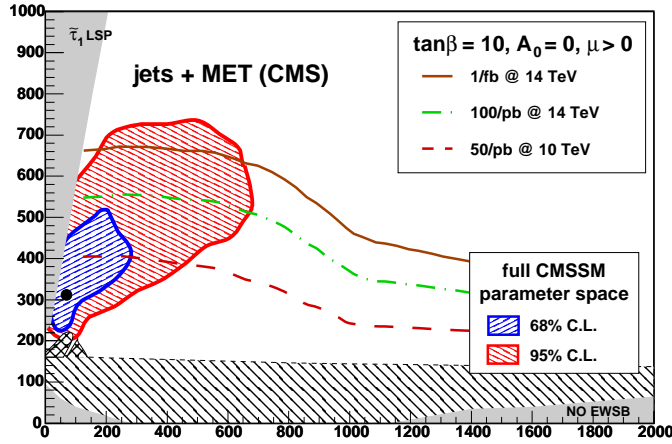


**Fig. 2** Regions of the  $(m_0, m_{1/2})$  plane favoured in a pre-LHC global frequentist analysis of the CMSSM at the 68% CL (blue) and the 95% CL (red), as well as the best-fit point (black) [15]. Overlaid are the reaches estimated by CMS for discovering supersymmetry within the CMSSM, with the indicated amounts of luminosity and centre-of-mass energy. These estimates were made specifically for  $\tan \beta = 10$  and  $A_0$ , but apply more generally.

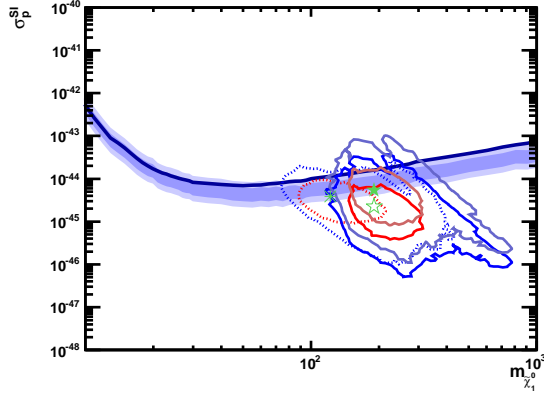


**Fig. 3** The correlation found in the CMSSM between the spin-independent dark matter scattering cross section  $\sigma_p^{SI}$  and the LSP mass  $m_{\tilde{\chi}_1^0}$  prior to the 2010 LHC data and the current Xenon100 results shown by dotted lines, red and blue for the 68 and 95% CL contours, respectively [17]. The solid lines include the 2010 LHC results: those calculated assuming  $\Sigma_{\pi N} = 50$  MeV are shown as brighter coloured curves and those for  $\Sigma_{\pi N} = 64$  MeV as duller coloured curves, in each case disregarding uncertainties. The green ‘snowflakes’ (open stars) (filled stars) are the best-fit points in the corresponding models. Also shown is the 90% CL Xenon100 upper limit [18] and its expected sensitivity band.

### 3 Astrophysical searches for supersymmetric dark matter

These include the direct search for elastic dark matter scattering on a nucleus in the laboratory,  $\chi + N \rightarrow \chi + N$ , indirect searches for  $\chi\chi$  annihilations in the core of the Sun or Earth via energetic muons produced by energetic solar or terrestrial neutrinos, the indirect search for  $\chi\chi$  annihilations in the galactic centre or elsewhere via energetic  $\gamma$  rays, and indirect searches for  $\chi\chi$  annihilations in the galactic halo via antiprotons or positrons among the cosmic rays.

Pre-LHC predictions at the 68% and 95% CL for spin-independent elastic dark matter scattering cross section on a proton,  $\sigma_p^{SI}$ , are shown as dotted lines in Fig. 3 [17], and compared with the upper limit from the Xenon100 experiment [18] discussed below. We see that the best-fit prediction lies close to the current experimental sensitivity and within reach of prospective future experiments.

It should be noted, however, that these predictions are sensitive to the assumed value of the  $\pi$ -N scattering  $\sigma$  term,  $\Sigma_{\pi N}$ , as seen in Fig. 4 for the cases of some specific CMSSM benchmark scenarios [19]. This sensitivity arises because  $\Sigma_{\pi N}$  is sensitive to Higgs-exchange diagrams, which are sensitive, in turn, to the scalar density of strange quarks in the proton:  $\langle p | \bar{s}s | p \rangle$ . Estimating this requires comparing octet baryon mass differences, which yield a value for  $\sigma_0 \equiv \frac{1}{2}(m_u + m_d)\langle p | \bar{u}u + \bar{d}d - 2\bar{s}s | p \rangle = 36 \pm 7$  MeV, with  $\Sigma_{\pi N} = \frac{1}{2}(m_u +$

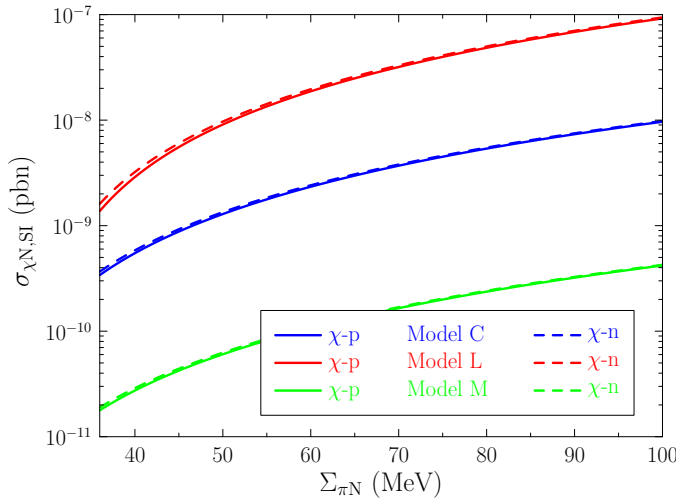


**Fig. 4** Spin-independent dark matter scattering cross sections  $\sigma_{p,n}^{SI}$  for three CMSSM benchmark models C, L, and M [19]. Note that  $\sigma_p^{SI}$  and  $\sigma_n^{SI}$  are nearly indistinguishable at the scale used in this plot.

$m_d)\langle p|\bar{u}u + \bar{d}d\rangle$ . The strangeness ratio  $y \equiv 2\langle p|\bar{s}s|p\rangle/\langle p|\bar{u}u + \bar{d}d\rangle = 1 - \sigma_0/\Sigma_{\pi N}$ . Some experiments suggest a relatively large value of  $\Sigma_{\pi N} \sim 64$  MeV or more [20], and hence that  $y$  is large, whereas some lattice calculations suggest that  $y$  is small [21]. Fig. 3 displays as brighter (duller) solid lines our post-2010-LHC predictions for  $\sigma_p^{SI}$  assuming  $\Sigma_{\pi N} = 50(64)$  MeV, demonstrating further the importance of pinning down  $\Sigma_{\pi N}$ . In the following, we assume that  $\Sigma_{\pi N} = 50 \pm 14$  MeV, commenting on the implications if a larger value is assumed.

#### 4 Implications of initial LHC searches for supersymmetry

The CMS [14] and ATLAS [12] Collaborations have both announced negative results from initial searches for supersymmetry using the  $\sim 35/\text{pb}$  of data each accumulated in 2010, and ATLAS has also released preliminary results from a search using  $\sim 165/\text{pb}$  of 2011 data [13]. Their implications for the CMSSM may be represented in  $(m_0, m_{1/2})$  planes that are insensitive to  $A_0$  and  $\tan\beta$ . As seen in Fig. 5, the most sensitive constraints are those from searches for jets accompanied by missing energy, which extend to much larger mass values than the previous Tevatron and LEP constraints on supersymmetry, as also seen in Fig. 5.

We have explored the implications of these data for supersymmetric models in an extension of the frequentist global analysis introduced earlier [14], including also the negative results of LHC searches for the heavier supersymmetric Higgs bosons  $H, A$  [22] and also upper limits on  $B_s \rightarrow \mu^+\mu^-$  decay

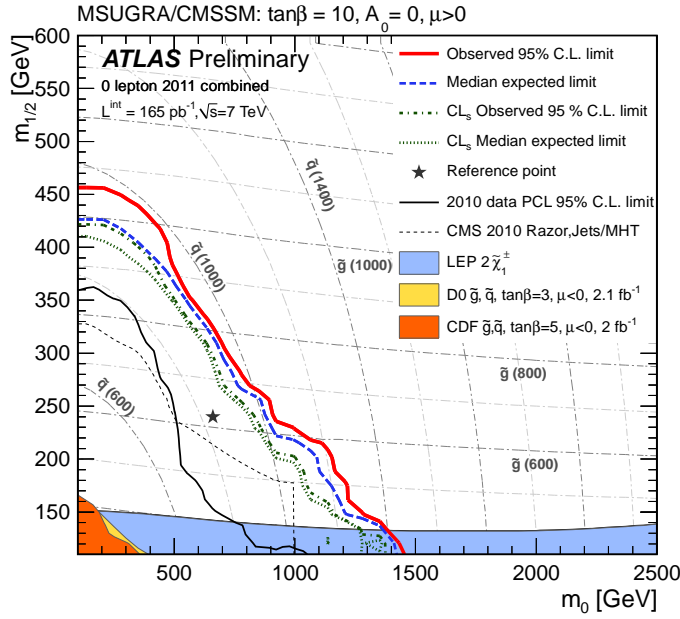


**Fig. 5** Compilation of ATLAS and CMS 95% CL exclusion limits in the  $(m_0, m_{1/2})$  plane of the CMSSM. The ATLAS limit obtained with 165/pb of 2011 data, assuming  $\tan\beta = 10$ ,  $A_0 = 0$  and  $\mu > 0$  and using the PCL ( $CL_s$ ) method is shown as a solid red (dot-dashed green) line, also shown are the corresponding expected limits and a reference point [13]. The CMS [14] and ATLAS [12] limits from 2010 LHC data assuming  $\tan\beta = 3$  are shown as dashed and solid black lines, respectively. Also shown for illustration are limits from the Tevatron and from LEP.

from the LHCb [23], CDF [24] and D0 [25] experiments. Fig. 6 compares the best-fit points, 68% and 95% CL regions in the CMSSM before and after including the 2010 LHC data. We see that the best-fit point has moved to larger  $m_{1/2}$ , in particular, but still lies within the pre-LHC 68% CL region. Thus is not yet significant tension with the pre-LHC predictions.

## 5 The Xenon100 direct dark matter search experiment

The Xenon100 experiment has recently announced results from an analysis of 100 days of data, establishing an upper limit on the spin-independent dark matter scattering cross section  $\sigma_p^{SI}$  that is significantly lower than those from previous experiments [18]. As seen in Fig. 3, this is the first dark matter scattering experiment that impinges significantly on the expected parameter space of simple supersymmetric models such as the CMSSM. However, the confrontation with CMSSM predictions must take into account the uncertainties in the spin-independent hadronic scattering matrix element, primarily those related to  $\Sigma\pi_N$  that were discussed earlier. Fig. 7 shows the results of including the

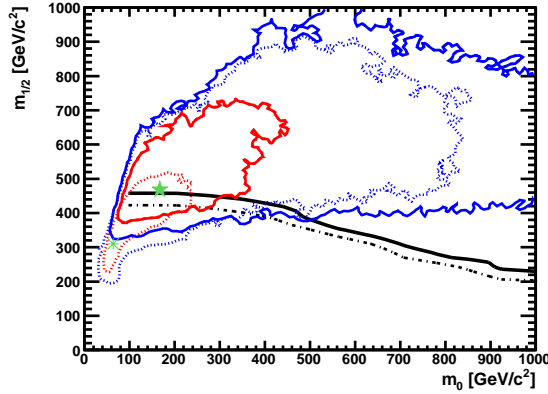


**Fig. 6** The  $(m_0, m_{1/2})$  plane in the CMSSM showing the regions favoured pre-LHC (dotted lines) and after including all the 2010 LHC data as well as the Xenon100 limit (solid lines) at the 68% CL (red) and at the 95% CL (blue) [17]. Also shown in green are the pre- and post-2010-LHC/Xenon100 best-fit points, and the preliminary 95% CL limits obtained by ATLAS using 165/pb of 2011 data using a PCL approach (solid black line) and a  $CL_s$  approach (dash-dotted black line) [13].

Xenon100 results in the global CMSSM fit [17], assuming the default option  $\Sigma_{\pi N} = 50 \pm 14$  MeV (brighter colours). The main effect of a larger value for  $\Sigma_{\pi N}$  would be to increase the lower bound on  $\sigma_p^{SI}$ , typically by a factor  $\sim 3$  if  $\Sigma_{\pi N} = 64 \pm 8$  MeV (duller colours).

## 6 Indirect Strategies for Detecting Supersymmetric Dark Matter

These centre on searches for the products of dark matter annihilations at low relative velocities, so the signals are all strongly dependent on the S-wave annihilation cross section. Values along the WMAP strips for  $\tan \beta = 10$  and 55 are shown in Fig. 8 [6]. We see that the cross section is generally much smaller along the coannihilation strip for  $\tan \beta = 10$  than along the corresponding focus-point strip, or along both the WMAP strips for  $\tan \beta = 55$ . Thus the latter strips offer *a priori* better prospects the indirect detection of supersymmetric dark matter. Discussions of indirect search strategies sometimes focus on annihilation final states with particularly striking signatures such as  $\chi\chi \rightarrow \gamma\gamma$ . The relative annihilation rates can be calculated in the CMSSM, as seen in Fig. 9 [6]. We see that the  $\tau^+\tau^-$ ,  $W^+W^-$  and  $\bar{b}b$  final states dominate in general, and that the  $\gamma\gamma$  fraction is unfortunately very small in the CMSSM.



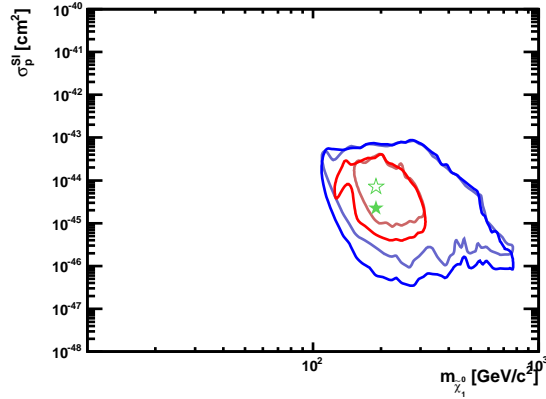


**Fig. 7** The correlation found in the CMSSM between the spin-independent dark matter scattering cross section  $\sigma_p^{SI}$  and the LSP mass  $m_{\tilde{\chi}_1^0}$  after including the constraints from the 2010 LHC data and the Xenon100 results, in red and blue for the 68 and 95% CL contours, respectively [17]. Those calculated assuming  $\Sigma_{\pi N} = 50 \pm 14$  MeV are shown as brighter coloured curves and those for  $\Sigma_{\pi N} = 64 \pm 8$  MeV as duller coloured curves. The green filled (open) star is the best-fit point for the corresponding range of  $\Sigma_{\pi N}$ .

### 6.1 Neutrino fluxes from dark matter annihilation in the Sun

Dark matter particles passing through the Sun or Earth may scatter, lose energy and become gravitationally bound. These bound dark matter particles may then annihilate, producing energetic neutrinos that generate detectable high-energy neutrinos when they interact with matter in or near a detector. It has often been assumed that the capture and annihilation processes are in equilibrium, but this is not the case in the CMSSM in general, as seen for the  $(m_{1/2}, m_0)$  plane with  $\tan\beta = 10$  in the left panel of Fig. 10 [26]. It has also often been thought that the dominant scattering mechanism in the Sun is spin-dependent scattering on protons, but in studies of the CMSSM we have found that the dominant role may actually be played by spin-independent scattering on heavier nuclei such as  $^4\text{He}$ , as seen in the right panel of Fig. 10 [26].

Fig. 11 shows the resulting neutrino fluxes above various neutrino energy thresholds along the WMAP strips in the CMSSM for  $\tan\beta = 10$  and 55, compared with the possible sensitivity of the IceCube/DeepCore detector [26]. The best prospects for detection are along the focus-point strip for  $\tan\beta = 10$ , where the neutrino flux might be detectable in IceCube/DeepCore out to  $m_\chi \sim 400$  GeV. On the other hand, the prospects are quite unpromising along the corresponding coannihilation strip, as one might have anticipated from the annihilation cross section plot in Fig. 8. In the case of  $\tan\beta = 55$ , there may be some prospects for neutrino detection for small values of  $m_\chi$  along the focus-point strip.

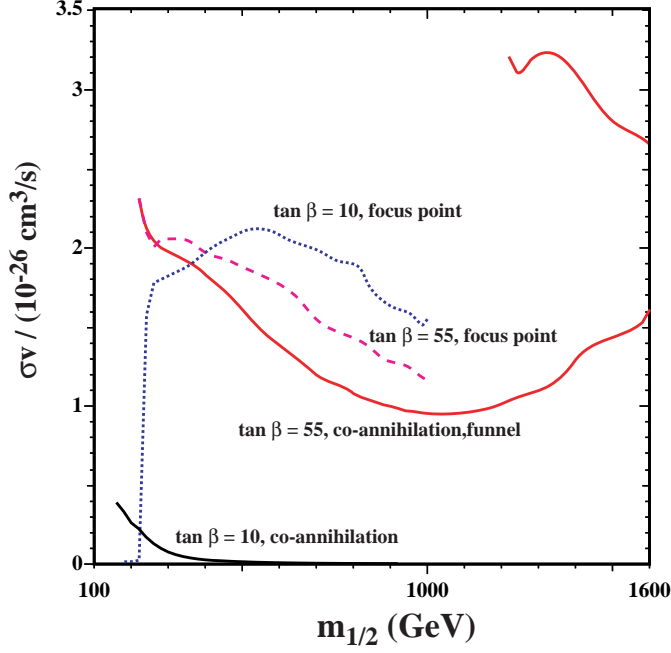


**Fig. 8** The LSP-LSP annihilation cross section along the WMAP strips in the coannihilation, focus-point and funnel regions for  $\tan \beta = 10, 55$ ,  $A_0 = 0$  and  $\mu > 0$ , as functions of  $m_{1/2}$ . We see that the annihilation cross section along the  $\tan \beta = 10$  coannihilation strip is much smaller than along the other strips, and decreases rapidly as  $m_{1/2}$  increases [6].

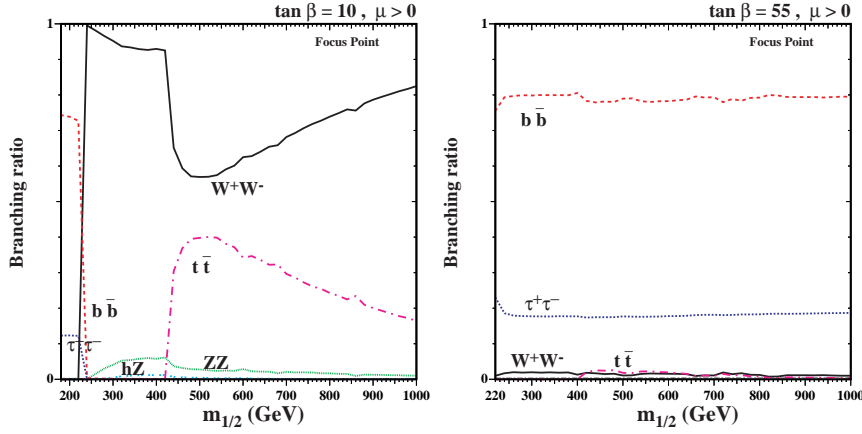


**Fig. 9** The branching fractions for LSP-LSP annihilations into pairs of Standard Model particles along the WMAP strips in the focus-point regions for  $\tan \beta = 10$  (left) and  $\tan \beta = 55$  (right) [6].

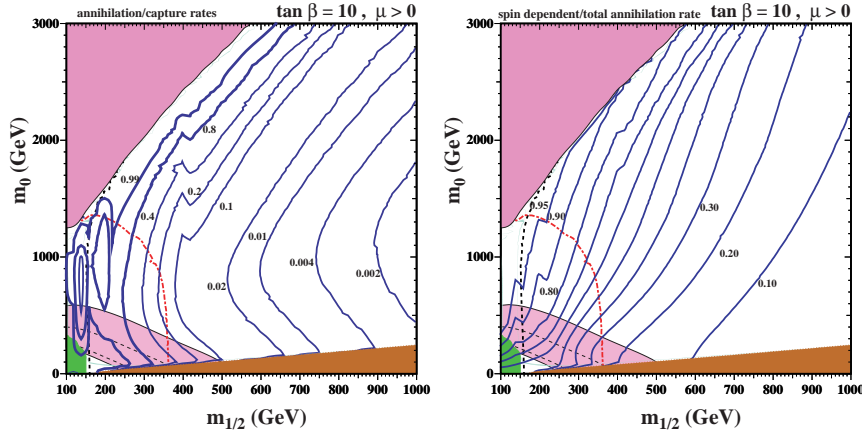


**Fig. 10** The  $(m_{1/2}, m_0)$  plane in the CMSSM for  $A_0 = 0$  and  $\tan\beta = 10$ , showing, in the left panel, contours of the ratio of solar dark matter annihilation and capture rates, as calculated using default values of the hadronic scattering matrix elements [26]. Equilibrium corresponds to a ratio of unity, which is approached for small  $m_{1/2}$  and large  $m_0$ . The right panel shows contours of the ratio of the solar dark matter annihilation rate calculated using only spin-dependent scattering to the total annihilation rate including also spin-independent scattering [26]. It is seen that spin-independent scattering is important, even dominant, in much of the plane.

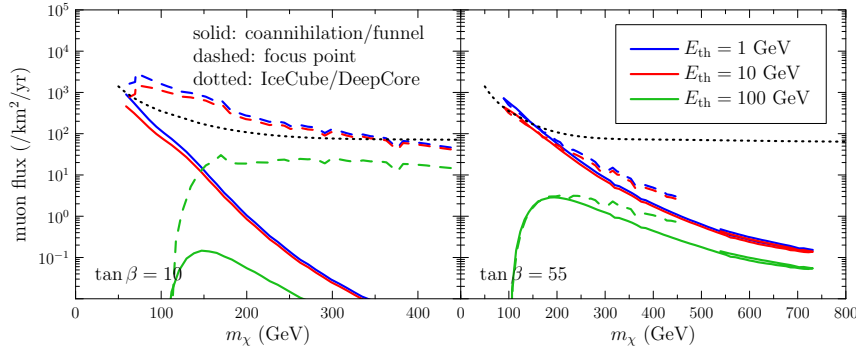


**Fig. 11** The CMSSM muon fluxes through a detector calculated for  $A_0 = 0$  and (left)  $\tan\beta = 10$ , (right)  $\tan\beta = 55$ , along the WMAP strips in the coannihilation/funnel regions (solid) and the focus-point region (dashed) [26]. Fluxes are shown for muon energy thresholds of (top to bottom) 1 GeV, 10 GeV, and 100 GeV. Also shown is a conservative estimate of the sensitivity of the IceCube/DeepCore detector (dotted), normalized to a muon threshold of 1 GeV, for a particular hard annihilation spectrum ( $\tau\bar{\tau}$  for  $m_\chi < 80$  GeV,  $W^+W^-$  at higher masses). The IceCube/DeepCore sensitivity shown does not directly apply to the CMSSM flux curves, but can be treated as a rough approximation to which CMSSM models might be detectable.

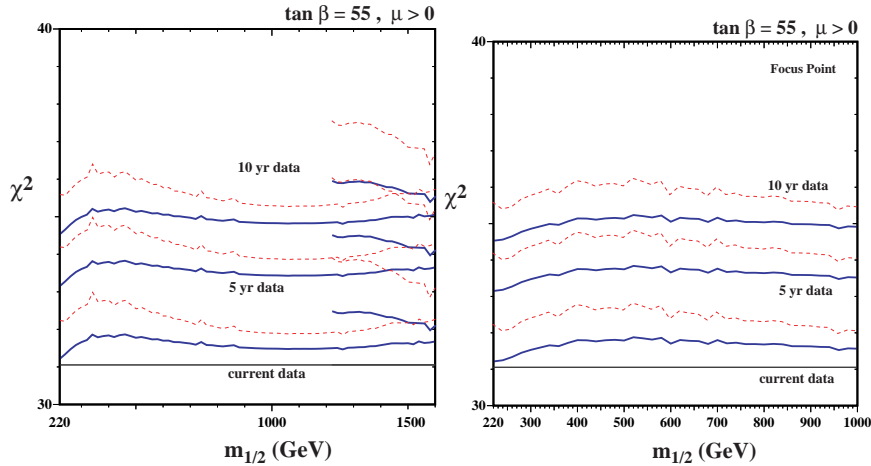


**Fig. 12** The  $\chi^2$  functions along the CMSSM WMAP strips as functions of  $m_{1/2}$  for  $\tan\beta = 55$ , along the coannihilation/funnel strip (left panel) and in the focus-point region (right panel) [6]. In each panel, we display the  $\chi^2$  function for the background alone as a horizontal line at  $\chi^2 = 31.1$ , the  $\chi^2$  function obtained by adding the calculated LSP-LSP annihilation signal in the current (approximately 2 1/2 year) Fermi data sample [29], and in projected 5- and 10-year data sets. Solid (blue) curves are based on an NFW profile [27], while dashed (red) curves are based on an Einasto profile [28].

## 6.2 Gamma-ray fluxes from dark matter annihilation in the Galactic core

Many studies have been made of the detectability of high-energy  $\gamma$  rays produced by the annihilations of dark matter particles in the core of the Milky Way, in the Galactic bulge, in dwarf galaxies, and in the diffuse cosmic background. Fig. 12 displays the possible sensitivity of the Fermi-LAT detector to  $\gamma$  rays from dark matter annihilations in the Galactic core along the coannihilation and focus-point strip in the CMSSM with  $\tan\beta = 55$  [6]. There is an important uncertainty associated with the dark matter density profile in the core, and results are shown for a Navarro-Frenk-White (NFW) profile [27] (solid blue lines) and for an Einasto [28] profile (dashed red lines). The lowest sets of lines in Fig. 12 indicate the increase in  $\chi^2$  that might arise from a dark matter annihilation contribution, relative to a fit to the current Fermi-LAT data [29] in the absence of any supersymmetric signal, which corresponds to the horizontal solid black line with  $\chi^2 = 31.1$ . The higher sets of lines indicate what might be possible with 5- and 10-year Fermi-LAT data sets: in these cases the values of  $\chi^2$  in the absence of a supersymmetric signal would be  $\sim 33.0$  and  $34.3$ , respectively.

The sensitivity of the Fermi-LAT experiment could be increased significantly with improvements in the understanding of the background and the systematic uncertainty in the area of the detector. Fig. 13 indicates the discrimination that could be possible if the background could be understood with

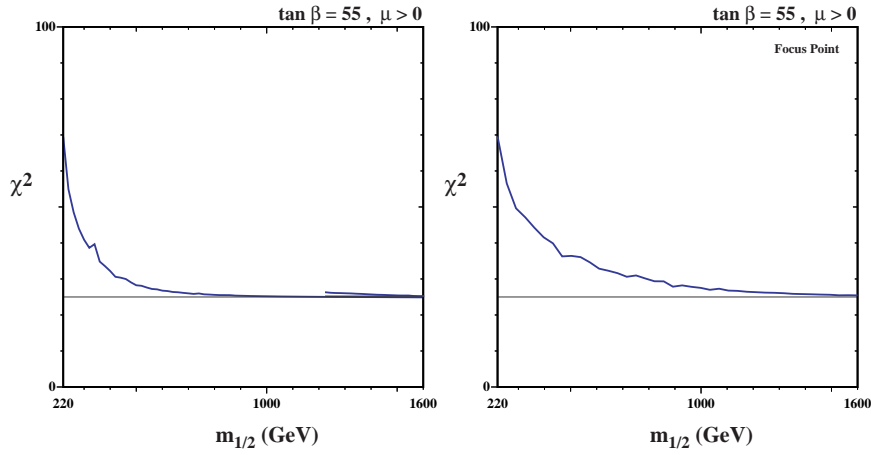


**Fig. 13** The  $\chi^2$  functions as functions of  $m_{1/2}$  along the CMSSM focus-point WMAP strip for  $\tan \beta = 55$  assuming a negligible systematic error, assuming that an improved estimate of the background brings it to  $\pm 1\sigma$  from the data [6]. The left (right) panel is for the coannihilation/funnel strip (focus-point strip).

random errors of  $\pm 1\sigma$  relative to the measurement, and the systematic error could be reduced to a negligible level. The blue lines assume an NFW profile, and the sensitivity would be substantially increased if the core had an Einasto profile.

### 6.3 Anomalies in $e^\pm$ spectra?

A couple of surprising features have been observed in the  $e^\pm$  spectra in the cosmic rays. One is a shoulder in the sum of the  $e^+$  and  $e^-$  spectra between  $\sim 100$  and  $1000$  GeV [30], and the other is an increase in the  $e^+/e^-$  ratio between  $\sim 10$  and  $100$  GeV [31]. Before jumping to an interpretation involving the annihilations of dark matter particles, one should first consider more prosaic interpretations, taking into account uncertainties in cosmic-ray production and propagation through the galaxy, as well as possible contributions from nearby sources. These may render unnecessary an explanation in terms of dark matter annihilations, which would in any case require a rather special supersymmetric model.

### 6.4 Antiprotons and antideuterons from dark matter annihilations?

The spectrum of cosmic-ray antiprotons has now been measured quite accurately, and at energies  $< 10$  GeV it seems to agree well with calculations of the production of secondary antiprotons by primary matter cosmic rays [32]. However, there may be some discrepancy at higher energies, that could possibly be

due to dark matter annihilations, though a more conservative interpretation in terms of primary antimatter production by cosmic-ray sources is also possible. Another possible signal of dark matter annihilations may be provided by antideuterons with energies below about 1 GeV [33], which may be distinguishable from conventional antideuteron mechanisms that give a spectrum peaked at energies  $> 1$  GeV.

## 6.5 AMS

The AMS experiment was launched successfully shortly after this talk, and subsequently placed on the International Space Station [34]. We hope that it will be able cast light on the dark mysteries mentioned in the two previous subsections!

## 7 Final Remarks

Hopefully this talk has convinced you that, on the one hand, the LHC may soon be casting light on the nature of dark matter while, on the other hand, astrophysical experiments may soon be casting light on fundamental questions in particle physics. Only the synthesis between the two will have any chance of determining the true nature of dark matter. Please also recall that important contributions to unravelling this physics may be played by humble low-energy experiments, e.g., on  $\pi - N$  scattering and pionic atoms, that may remove crucial uncertainties in this synthesis. Please also note the important roles that may be played by antiparticles, including antideuterons and positrons, as well as antiprotons. Finally, be ready for the unexpected! We should all hope that the LHC will become famous for discovering some unforeseen physics, and be open to the possibility that some unheralded experiment will make the crucial discovery leading to a breakthrough in the understanding of dark matter.

## References

1. M. Bustamante, L. Cieri and J. Ellis, *Beyond the Standard Model for Montaneros*, arXiv:0911.4409 [hep-ph].
2. H. Goldberg, *Constraint on the Photino Mass from Cosmology*, Phys. Rev. Lett. **50**, 1419 (1983) [Erratum-ibid. **103**, 099905 (2009)]; J. R. Ellis, J. S. Hagelin, D. V. Nanopoulos, K. A. Olive and M. Srednicki, *Supersymmetric Relics from the Big Bang*, Nucl. Phys. B **238**, 453 (1984).
3. H. E. Haber and G. L. Kane, *The Search for Supersymmetry: Probing Physics Beyond the Standard Model*, Phys. Rept. **117**, 75 (1985).
4. G. L. Kane, C. F. Kolda, L. Roszkowski and J. D. Wells, *Study of constrained minimal supersymmetry*, Phys. Rev. D **49**, 6173 (1994) [arXiv:hep-ph/9312272].
5. J. R. Ellis, K. A. Olive, Y. Santoso and V. C. Spanos, *Supersymmetric dark matter in light of WMAP*, Phys. Lett. B **565**, 176 (2003) [arXiv:hep-ph/0303043].
6. J. Ellis, K. A. Olive and V. C. Spanos, *Galactic-Centre Gamma Rays in CMSSM Dark Matter Scenarios*, arXiv:1106.0768 [hep-ph].

7. Joint Supersymmetry Working Group of the ALEPH, DELPHI, L3 and OPAL Experiments, <http://lepsusy.web.cern.ch/lepsusy/>.
8. K. Nakamura *et al.* (Particle Data Group) *Review of Particle Physics*, J. Phys. G **37**, 075021 (2010).
9. LEP Higgs Working Group, <http://lephiggs.web.cern.ch/LEPHIGGS/www/Welcome.html>.
10. G. W. Bennett *et al.* [Muon G-2 Collaboration], *Final Report of the Muon E821 Anomalous Magnetic Moment Measurement at BNL*, Phys. Rev. D **73**, 072003 (2006) [arXiv:hep-ex/0602035].
11. E. Komatsu *et al.* [WMAP Collaboration], *Seven-Year Wilkinson Microwave Anisotropy Probe (WMAP) Observations: Cosmological Interpretation*, Astrophys. J. Suppl. **192**, 18 (2011) [arXiv:1001.4538 [astro-ph.CO]].
12. G. Aad *et al.* [ATLAS Collaboration], *Combined exclusion reach of searches for squarks and gluinos using final states with jets, missing transverse momentum, and zero or one lepton, with the ATLAS detector in  $\sqrt{s}=7$  TeV proton-proton collisions*, <http://cdsweb.cern.ch/record/1345745> (2011).
13. G. Aad *et al.* [ATLAS Collaboration], *Search for squarks and gluinos using final states with jets and missing transverse momentum with the ATLAS detector in  $\sqrt{s}=7$  TeV proton-proton collisions*, <http://cdsweb.cern.ch/record/1356194> (2011).
14. S. Chatrchyan *et al.* [CMS Collaboration], *Search for new physics at CMS with jets and missing momentum*, <http://cdsweb.cern.ch/record/1343076> (2011).
15. O. Buchmueller *et al.*, *Predictions for Supersymmetric Particle Masses using Indirect Experimental and Cosmological Constraints*, JHEP **0809**, 117 (2008) [arXiv:0808.4128 [hep-ph]].
16. O. Buchmueller *et al.*, *Likelihood Functions for Supersymmetric Observables in Frequentist Analyses of the CMSSM and NUHM1*, Eur. Phys. J. C **64**, 391 (2009) [arXiv:0907.5568 [hep-ph]]; *Frequentist Analysis of the Parameter Space of Minimal Supergravity*, Eur. Phys. J. C **71**, 1583 (2011) [arXiv:1011.6118 [hep-ph]]; Eur. Phys. J. C **71**, 1634 (2011) [arXiv:1102.4585 [hep-ph]].
17. O. Buchmueller *et al.*, *Supersymmetry and Dark Matter in Light of LHC 2010 and Xenon100 Data*, arXiv:1106.2529 [hep-ph].
18. E. Aprile *et al.* [XENON100 Collaboration], *Dark Matter Results from 100 Live Days of XENON100 Data*, arXiv:1104.2549 [astro-ph.CO].
19. J. R. Ellis, K. A. Olive and C. Savage, *Hadronic Uncertainties in the Elastic Scattering of Supersymmetric Dark Matter*, Phys. Rev. D **77**, 065026 (2008) [arXiv:0801.3656 [hep-ph]].
20. M. M. Pavan, I. I. Strakovsky, R. L. Workman and R. A. Arndt, *The Pion nucleon Sigma term is definitely large: Results from a G.W.U. analysis of  $\pi$ -nucleon scattering data*, PiN Newslett. **16** (2002) 110 [arXiv:hep-ph/0111066]; M. M. Pavan, private communication (2011), taking into account recent data on pionic Deuterium: see T. Strauch *et al.*, *Pionic deuterium*, arXiv:1011.2415 [nucl-ex], as interpreted in V. Baru, C. Hanhart, M. Hoferichter, B. Kubis, A. Nogga and D. R. Phillips, *Precision calculation of the  $\pi^-$  deuteron scattering length and its impact on threshold  $\pi$ -N scattering*, arXiv:1003.4444 [nucl-th].
21. R. D. Young and A. W. Thomas, *Octet baryon masses and sigma terms from an  $SU(3)$  chiral extrapolation*, Phys. Rev. D **81** (2010) 014503 [arXiv:0901.3310 [hep-lat]].
22. G. Aad *et al.* [ATLAS Collaboration], <http://cdsweb.cern.ch/record/1336757/files/ATLAS-CONF-2011-024.pdf>; S. Chatrchyan *et al.* [CMS Collaboration], *Search for Neutral MSSM Higgs Bosons Decaying to Tau Pairs in  $pp$  Collisions at  $\sqrt{s} = 7$  TeV*, arXiv:1104.1619 [hep-ex].
23. R. Aaij *et al.* [LHCb Collaboration], *Search for the rare decays  $B_s \rightarrow \mu^+ \mu^-$  and  $B_d \rightarrow \mu^+ \mu^-$* , Phys. Lett. B **699**, 330 (2011) [arXiv:1103.2465 [hep-ex]].
24. T. Aaltonen *et al.* [CDF Collaboration], *Search for  $B_s^0 \rightarrow \mu^+ \mu^-$  and  $B^0 \rightarrow \mu^+ \mu^-$  Decays with 2/fb of  $p\bar{p}$  Collisions*, Phys. Rev. Lett. **100**, 101802 (2008) [arXiv:0712.1708 [hep-ex]]; see also [http://www-cdf.fnal.gov/physics/new/bottom/090813\\_blessed-Bsd2mumu/bsmumupub3.7fb\\_v01.pdf](http://www-cdf.fnal.gov/physics/new/bottom/090813_blessed-Bsd2mumu/bsmumupub3.7fb_v01.pdf).
25. V. M. Abazov *et al.* [D0 Collaboration], *Search for the rare decay  $B_s^0 \rightarrow \mu^+ \mu^-$* , Phys. Lett. B **693** 539 (2010) [arXiv:1006.3469 [hep-ex]].
26. J. Ellis, K. A. Olive, C. Savage and V. C. Spanos, *Neutrino Fluxes from CMSSM LSP Annihilations in the Sun*, Phys. Rev. D **81**, 085004 (2010) [arXiv:0912.3137 [hep-ph]].

27. J. F. Navarro, C. S. Frenk and S. D. M. White, *A Universal density profile from hierarchical clustering*, *Astrophys. J.* **490**, 493 (1997) [arXiv:astro-ph/9611107].
28. J. Einasto, *Influence of the atmospheric and instrumental dispersion on the brightness distribution in a galaxy*, *Trudy Inst. Astrofiz. Alma-Ata* **51**, 87 (1965); J. Einasto and U. Haud, *Galactic models with massive corona*, *Astron. Astrophys.* **223**, 89 (1989); A. W. Graham, D. Merritt, B. Moore, J. Diemand, B. Terzic, *Empirical models for Dark Matter Halos. I. Nonparametric Construction of Density Profiles and Comparison with Parametric Models*, *Astron. J.* **132**, 2685 (2006), [astro-ph/0509417].
29. V. Vitale and A. Morselli, for the Fermi-LAT Collaboration, *Indirect Search for Dark Matter from the center of the Milky Way with the Fermi-Large Area Telescope*, arXiv:0912.3828 [astro-ph.HE].
30. M. Ackermann *et al.* [Fermi LAT Collaboration], *Fermi LAT observations of cosmic-ray electrons from 7 GeV to 1 TeV*, *Phys. Rev. D* **82**, 092004 (2010) [arXiv:1008.3999 [astro-ph.HE]], and references therein.
31. O. Adriani *et al.* [PAMELA Collaboration], *An anomalous positron abundance in cosmic rays with energies 1.5-100 GeV*, *Nature* **458**, 607 (2009) [arXiv:0810.4995 [astro-ph]].
32. O. Adriani *et al.* [PAMELA Collaboration], *PAMELA results on the cosmic-ray antiproton flux from 60 MeV to 180 GeV in kinetic energy*, *Phys. Rev. Lett.* **105**, 121101 (2010) [arXiv:1007.0821 [astro-ph.HE]].
33. Ph. von Doetinchem *et al.*, *The General Antiparticle Spectrometer (GAPS) - Hunt for dark matter using low-energy antideuteron*, arXiv:1012.0273 [astro-ph.IM].
34. AMS Collaboration, <http://www.ams02.org/>.